THEORETICAL AND EXPERIMENTAL ANALYSIS OF COMPOSITE BEAMS WITH ELASTIC COUPLINGS

Clemens Kaiser*, Chair for Lightweight-Structures, Technical University of Munich
Davide Francescatti**, Department of Aerospace-Engineering, University of Pisa

Abstract

A theory for linear analysis of thin-walled beams with open cross-section containing elastic couplings made of general composite laminates is developed.
For special fibre-reinforced materials with a low ratio $E_{\parallel}/E_{\perp}$ as glass-fibre-reinforced plastics a complex behaviour even of a single layer is to be found. Considering this and other non-classical effects like transverse-shear deformation the basic assumption of rigid cross-section for the calculation must be checked carefully.
Thus a known theory was modified by including the influence on the inplane-deformation of the cross-section, which is caused by the effects of elastic coupling of the laminated branches of the cross-section and by the strains in direction of the contour-line of the cross-section.
Finite-element-analysis as well as experimental results confirm the modified theory and at the same time show its limitations. Especially laminated beams with no or low proportion of fibres in axial direction can be exactly calculated with the modified theory and have a large deviation to results calculated with other theories. Beams containing segments of laminates with a high inplane coupling can not be exactly calculated, even with the modified theory.

Nomenclature

A_{ij}, B_{ij}, D_{ij}	membrane, coupling and plate stiffnesses
b, h, l	width, height and length of beam
B_T	warping bimoment
C_{ij}	single layer stiffness
$E_{\parallel}$, $E_{\perp}$	Young's moduli of plies, referring to fibre orientation
$G_{\#}$	shear modulus of plies
K_{ij}*	beam stiffnesses
M_y, M_z	bending moments, referring to beam
$\bar{M}_T$	applied torsion moment
M_T	torsion moment, referring to beam
m_x, m_s, m_{xs}	bending and twisting moments
N	axial force, referring to beam
n_x, n_s, n_{xs}	membrane forces
n, s, x	coordinate system for plate segment
$\bar{Q}$	applied force
t	wall thickness
U, V, W	displacements of beam
u, v, w	displacements of plate segment
x, y, z	coordinate system for beam
α	fibre orientation
ε_x, ε_s, γ_{xs}	membrane strains referring to plate segments
ε_{xy}, ε_{xz}	transverse shear strain for beam
κ_x, κ_s, κ_{xs}	bending curvatures referring to plate segment
σ_x, σ_s, τ_{xs}	stress field referring to plate segement
φ_x, φ_y, φ_z	rotations around axes referring to beam
$\nu_{\parallel\perp}$	Poisson's ratio of plies
ω	warping function

Introduction

Composite materials are used in a wide field of applications for lightweight structures. Its technology allows the construction of specific material features by various ways of stacking differently orientated fibres in the plies. Quite usual is a symmetric and balanced stacking which results in orthotropic material behaviour. Deviation from this usual procedure leads to anisotropic material behaviour including so-called elastic couplings like tension-shear, tension-torsion or bending-torsion coupling.
In practice such anisotropic structures are usually not used. One reason for this may be compex methods of calculation methods, and another are the difficulties of reproducable production of anisotropic structures.
Today the potential of elastic couplings is recognized, because it is possible to take advantage of such couplings. Applications are being found referring to static or dynamic behaviour of composite rotor blades[1], influence of aero-elasticity of composite aircraft wings[2] or creation of coupled deformations with strain-actuators[3]. The numerical methods using finite-element-method allow simple and effective analysis of general anisotropic structures.
There are a lot of theories which have been developed for analytical calculation of the structural behaviour of thin-walled composite beams. Bauld and Tzeng[4] presented a theory derived from Vlasov's theory for thin-walled elastic beams[5] which was developed for isotropic material, but which does not take into account non-classical effects like transverse-shear deformation and coupling between laminate membrane reactions and moments.

* Scientific Research Assistant
** Student of Aeronautical Sciences

Chandra and Chopra[6] established a theory which includes these effects and obtained verification of this theory with experiments on composite I-beams containing unsymmetric laminate stackings. They expanded this theory[7] to a more complex theory with more generalized beam forces by considering inplane-warping effects. Wu and Sun[8] developed a theory including the inplane-warping effects by taking into account strains in contour direction of cross-section, but by using classical shell theory calculation procedure is also very complex.

In this paper a modified theory for calculation of thin-walled composite beams with elastic couplings is presented which bases on the Vlasov-type theory of Chandra and Chopra[6]. Besides consideration of transverse-shear deformation this theory takes into account the effects of inplane warping of cross-section and its influence on the structural behaviour which can be neglected only with specific composite beams as shown in this paper. This is realized by combining the assumptions of Wu and Sun[8] with the theory of Chandra and Chopra[6]. To validate the analytical results glass-fibre reinforced C-beams were analysed both numerical and experimental.

Some Remarks on Elastic Couplings

First of all some introductory remarks have to be made for understanding and interpreting the complex behaviour of composite beams with elastic couplings. The best way to do this is to look at the basic relationship between stress and strain of a single anisotropic layer (1).

$$\{\sigma_{xy}\} = [C]\cdot\{\varepsilon_{xy}\} \quad ; \quad \{\varepsilon_{xy}\} = [\overline{C}]\cdot\{\sigma_{xy}\}$$

$$\{\sigma_{xy}\} = \begin{Bmatrix}\sigma_x\\ \sigma_y\\ \tau_{xy}\end{Bmatrix} \quad ; \quad \{\varepsilon_{xy}\} = \begin{Bmatrix}\varepsilon_x\\ \varepsilon_y\\ \gamma_{xy}\end{Bmatrix} \qquad (1)$$

$$[\overline{C}]^T = [C]^{-1} \quad ; \quad [C] = \begin{bmatrix}C_{11} & C_{12} & C_{13}\\ C_{12} & C_{22} & C_{23}\\ C_{13} & C_{23} & C_{33}\end{bmatrix}$$

Several kinds of reinforced plastics were analysed for their coupling-behaviour[9]. To demonstrate the effects of elastic couplings the tension-shear-coupling of a glassfibre-reinforced-plastic (GRP) single layer is analysed here which material data is shown in table 1.

$E_\parallel$ [N/mm²]	$E_\perp$ [N/mm²]	$G_\#$ [N/mm²]	$\nu_{\parallel\perp}$
37940	11220	3300	0,24

Table 1: Material data for GRP

Refering to equation (1) the relationship between tension and coupled shear-deformation is:

$$\gamma_{xy} = \overline{C}_{13}\,\sigma_x = \frac{C_{12}C_{23} - C_{13}C_{22}}{\det|C|}\,\sigma_x \qquad (2)$$

All stiffness-coefficients C_{ij} of the single layer are enclosed in equation (2). Because of low ratio $E_\parallel/E_\perp$ of GRP the structural behaviour of tension-shear coupling is as shown in fig. 1. There is a change of sign at a fibre orientation of about 58 degrees, i.e. there is no tension-shear-coupling and, interestingly enough, the tension-stiffness is minimal (see fig. 3).

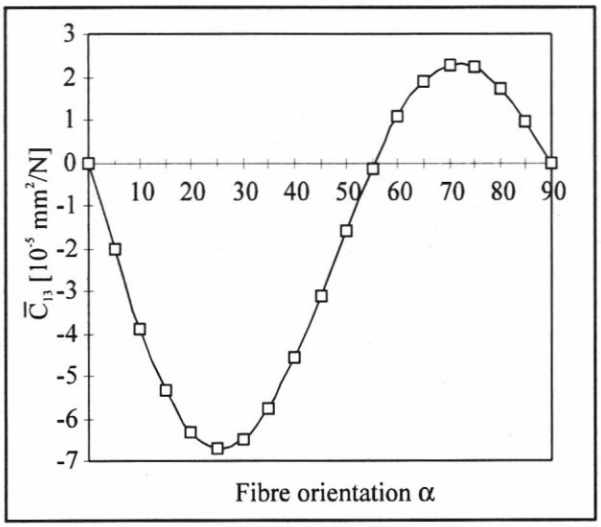

Fig. 1: Tension-shear coupling coeffizient $\overline{C}_{13}$ versus fibre orientation of a single GRP-layer

Such behaviour is not seen in carbon-fibre reinforced plastics (CRP) because of their high ratio $E_\parallel / E_\perp$.

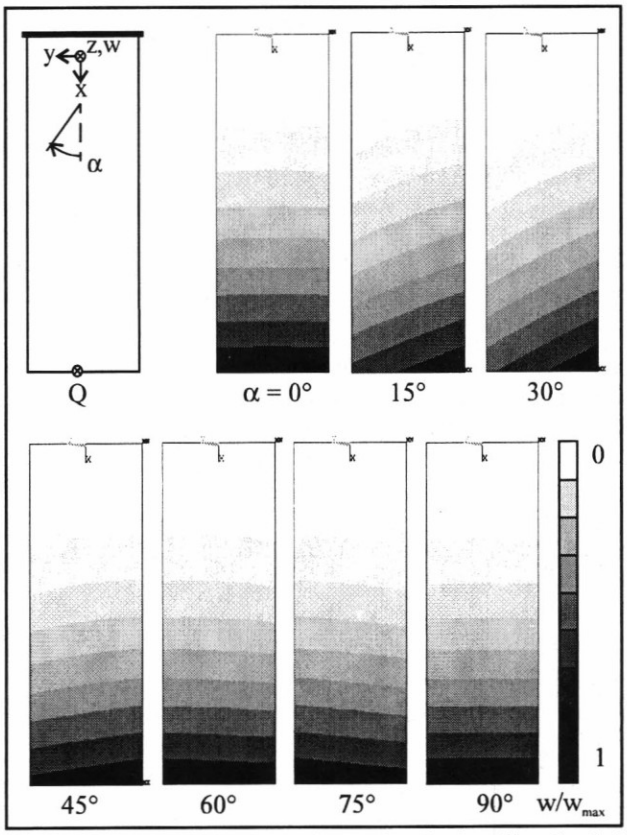

Fig.2: Bending-torsion coupling of a tip bending loaded GRP-plate with several fibre orientations

To show this effect of anisotropy a finite-element-analysis was made for tip bending loaded plates with homogeneous ply-stackings and several fibre-orientations. Because of this homogenity the resulting bending-torsion coupling is comparable to the tension-shear coupling described above (see fig. 2).
The result plots of relative displacement in z-direction shows the twisting behaviour of the GRP-plate depending on the fibre orientation. The curve of the lines indicates the coupling of bending load with deformation of the plate in its cross-section. For the single anisotropic layer one may conclude that a one-dimensional load leads to a complex two-dimensional strain. The tension-shear coupling is also influenced by the deformation perpendicular to the load direction. This simple connection is transferable to all elastic couplings of anisotropic structures. These findings are important for the modified theory for thin-walled composite beams.

Increase in stiffness by constraining deformation

In this paragraph the influence of constraining deformation on stiffness is analysed. Again the anisotropic single GRP layer serves as an example. From relation (1) tension stiffness can be calculated; the following relationship considers the boundary conditions $\sigma_y = \tau_{xy} = 0$:

$$\sigma_x = \frac{1}{\bar{C}_{11}} \varepsilon_x = \frac{\det|C|}{C_{22} C_{33} - C_{13}^2} \varepsilon_x = C_{11}^F \varepsilon_x \quad (3)$$

The coupled strain ε_y dependence on σ_x is:

$$\varepsilon_y = \bar{C}_{12} \sigma_x = \frac{C_{13} C_{23} - C_{12} C_{33}}{\det|C|} \sigma_x \quad (4)$$

(for γ_{xy} see relation (2)).
Considering the boundary conditions $\varepsilon_y = \gamma_{xy} = 0$, i.e. all deformations not in load-direction are constrained, relation (1) reduces to:

$$\sigma_x = C_{11} \varepsilon_x = C_{11}^C \varepsilon_x \quad (5)$$

and the induced stresses' σ_y and τ_{xy} dependence on σ_x can simply be calculated:

$$\sigma_y = \frac{C_{12}}{C_{11}} \sigma_x \quad ; \quad \tau_{xy} = \frac{C_{13}}{C_{11}} \sigma_x \quad (6)$$

In fig. 3 the variation of tension stiffnesses C_{11}^C (coupled displacements constrained) and C_{11}^F (free deformation) are shown depending on fibre orientation.
By constraining the coupled deformations a stiffness increase of up to 100% for the single layer is within reach when using GRP material. The increase is dependent on the magnitude of elastic coupling of the material. Such an increase is not seen in CRP, because of its smaller coupling behaviour as shown in the paragraph above. However, with an increase of stiffness additional stresses will be induced.

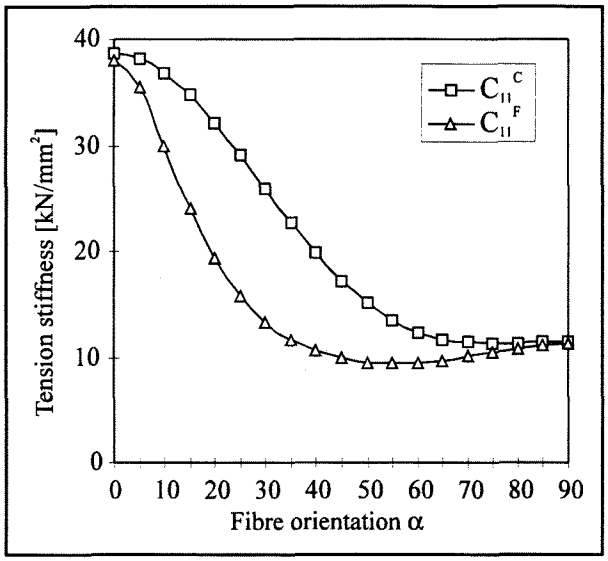

Fig. 3: Tension stiffnesses C_{11}^C (coupled deformations constrained) and C_{11}^F (free deformation) of a single GRP layer versus fibre orientation

Assumptions for the theory of thin-walled composite beams with elastic couplings

Most authors (like Chandra and Chopra[6][7], Wu and Sun[8] and Bauld and Tzeng[4]) base their theories on the theory of thin-walled beams by Vlasov[5] and Gjelsvik[10]. All these theories are based on the same fundamental assumptions. The reason for this is, that all these theories are developed from basic theories for isotropic material. Composite materials are different in some important aspects, but to apply the theories, a lot of assumptions made for isotropic materials can be transformed for composite materials.
Three basic assumptions are:
1) The cross-section of the beam does not deform in its own plane. This means inplane deformation of the cross-section is neglected and the strain in contour direction is neglected in comparison to the normal strain in direction of the beam-axis.
2) By doing that the normal stress in the contour direction is neglected in comparison to the normal stress in direction of the beam-axis.
3) The cross-section of the thin-walled beam consists of several straight segments. Any of these segments behave like a thin plate and are governed now by linear classical laminate theory.
Assumption 1) was introduced by Vlasov[5] and is valid for isotropic material. This assumption is important to formulate simple kinematic correlations for the cross-section. There are theories which take into account nonlinear kinematic effects[11] but they are limited to beams with solid cross-sections and very difficult to handle and change for thin-walled beams.
Beams of composite materials especially those with elastic couplings have a strange deformation-behaviour including a bigger inplane deformation of the cross-section than that of isotropic materials. The stacking sequence and fibre

orientation of the laminates is decisive for the inplane-behaviour. Using a high proportion of 0°-plies causes a high stiffness against inplane deformation. A good theory for composite beams should satisfy all variations of laminates. This leads automatically to a better understanding of the complex properties of composite materials.

Chandra and Chopra[6] have used CRP I-beams with stacking sequences $[0/90]_4$ in the web and $[0/90]_3$ in flanges with two layers of different fibre orientations at the bottom and on the top to get an anisotropic behaviour of the I-beam. The specimens used in this analysis are GRP C-beams with different fibre orientations $[+\alpha]_4$ or $[+\alpha/-\alpha]_S$ to show the limitations of the theories and their fundamental assumptions.

A finite-element-analysis of a tip bending loaded C-beam with stacking $[+45]_4$ shows a high inplane deformation (fig. 4) at the modelled ideal fixed bearing end (that means the beam can deform in its own plane at this end). Fig. 4 is not true to scale to get a better image of the inplane deformation.

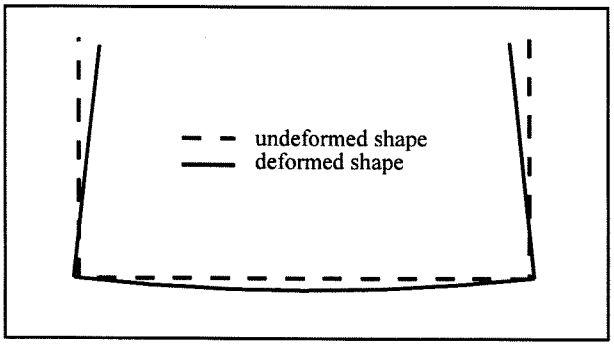

Fig. 4: C-beam under tip bending load. Qualitative deformation of cross-section at the ideal clamped end (not true to scale).

This is an indication that the validity for assumption 1) must always be checked.

Modified Plate Stress Field

The plate stress field of a general composite laminate including all strains and resulting moments is:

$$\begin{Bmatrix} n_x \\ n_y \\ n_{xy} \\ m_x \\ m_y \\ m_{xy} \end{Bmatrix} = \left[\begin{array}{c|c} A & B \\ \hline B & D \end{array}\right] \begin{Bmatrix} \varepsilon_x \\ \varepsilon_y \\ \gamma_{xy} \\ \kappa_x \\ \kappa_y \\ \kappa_{xy} \end{Bmatrix}; \quad [A] = \begin{bmatrix} A_{11} & A_{12} & A_{13} \\ A_{12} & A_{22} & A_{23} \\ A_{13} & A_{23} & A_{33} \end{bmatrix} \tag{7}$$

$$[B] = \begin{bmatrix} B_{11} & B_{12} & B_{13} \\ B_{12} & B_{22} & B_{23} \\ B_{13} & B_{23} & B_{33} \end{bmatrix}; \quad [D] = \begin{bmatrix} D_{11} & D_{12} & D_{13} \\ D_{12} & D_{22} & D_{23} \\ D_{13} & D_{23} & D_{33} \end{bmatrix}$$

A_{ij}, B_{ij} and D_{ij} are defined in the appendix.

The simplest way to take into account assumption 1) and 2) and neglect ε_y, κ_y, n_y and m_y is to eliminate line and row 2 and 5 of equation (7). By doing that the coupling effects induced by the strains ε_y and κ_y will be neglected. This plate stress field is used by Chandra and Chopra in their theory[6].

By skillfull convertation of equation (7) it is possible to fulfill assumptions 1) and 2) and take into account the induced influence of ε_y and κ_y on the other strains. It is assumed that the normal stresses in direction of the contour line (corresponding to n_y and m_y) are zero. The normal strains ε_y and κ_y are so small as to be neglected regarding to the inplane deformation. This is important to fulfill assumption 1) and to use the known kinematic correlations. But with regard to their influence on other strains they are not small. This assumption was made by Wu and Sun[8] and is used here in combination with the theory of Chandra and Chopra[6].

With condition n_y and m_y are zero in equation (7) ε_y in line 2 and κ_y in line 5 are described in dependency on ε_x, γ_{xy}, κ_x and κ_{xy}. These two correlations are substituted in the other four lines and one gets:

$$\begin{Bmatrix} n_x \\ n_{xy} \\ m_x \\ m_{xy} \end{Bmatrix} = \left[\begin{array}{c|c} A^* & B^* \\ \hline B^{*T} & D^* \end{array}\right] \begin{Bmatrix} \varepsilon_x \\ \gamma_{xy} \\ \kappa_x \\ \kappa_{xy} \end{Bmatrix}; \quad [A^*] = \begin{bmatrix} A_{11}^* & A_{13}^* \\ A_{13}^* & A_{33}^* \end{bmatrix} \tag{8}$$

$$[B^*] = \begin{bmatrix} B_{11}^* & B_{13}^* \\ B_{31}^* & B_{33}^* \end{bmatrix}; \quad [D^*] = \begin{bmatrix} D_{11}^* & D_{13}^* \\ D_{13}^* & D_{33}^* \end{bmatrix}$$

with

$$A_{11}^* = A_{11} + \frac{2A_{12}B_{12}B_{22} - A_{12}^2D_{22} - B_{12}^2A_{22}}{D_{22}A_{22} - B_{22}^2}$$

$$A_{13}^* = A_{13} + \frac{A_{12}(B_{22}B_{23} - A_{23}D_{22}) + B_{12}(A_{23}B_{22} - A_{22}B_{23})}{D_{22}A_{22} - B_{22}^2}$$

$$A_{33}^* = A_{33} + \frac{2A_{23}B_{22}B_{23} - A_{23}^2D_{22} - B_{23}^2A_{22}}{D_{22}A_{22} - B_{22}^2}$$

$$B_{11}^* = B_{11} + \frac{A_{12}(B_{22}D_{12} - B_{12}D_{22}) + B_{12}(B_{12}B_{22} - A_{22}D_{12})}{D_{22}A_{22} - B_{22}^2}$$

$$B_{13}^* = B_{13} + \frac{A_{12}(B_{22}D_{23} - B_{23}D_{22}) + B_{12}(B_{22}B_{23} - A_{22}D_{23})}{D_{22}A_{22} - B_{22}^2}$$

$$B_{31}^* = B_{13} + \frac{A_{23}(B_{22}D_{12} - B_{12}D_{22}) + B_{23}(B_{12}B_{22} - A_{22}D_{12})}{D_{22}A_{22} - B_{22}^2}$$

$$B_{33}^* = B_{33} + \frac{A_{23}(B_{22}D_{23} - B_{23}D_{22}) + B_{23}(B_{22}B_{23} - A_{22}D_{23})}{D_{22}A_{22} - B_{22}^2}$$

$$D_{11}^* = D_{11} + \frac{2B_{12}B_{22}D_{12} - B_{12}^2D_{22} - D_{12}^2A_{22}}{D_{22}A_{22} - B_{22}^2}$$

$$D_{13}^* = D_{13} + \frac{B_{12}(B_{22}D_{23} - B_{23}D_{22}) + D_{12}(B_{22}B_{23} - A_{22}D_{23})}{D_{22}A_{22} - B_{22}^2}$$

$$D_{33}^* = D_{33} + \frac{2B_{22}B_{23}D_{23} - B_{23}^2D_{22} - D_{23}^2A_{22}}{D_{22}A_{22} - B_{22}^2}$$

It is to be noted that the submatrix [B^*] is not symmetric any more and consists of four different stiffnesses. The whole stiffness-matrix, however, is symmetric.
This modified plate stress field (8) will be applied to the theory of Chandra and Chopra[6] to get better results for composite thin-walled beams containing a low inplane-deformation stiffness. The results will be compared to the results obtained with the original theory.

Theory of thin-walled composite beams with open cross-section and elastic coupings by Chandra and Chopra

The theory of Chandra and Chopra is based on the theory of Vlasov and Gjelsvik as mentioned above. The derivation of the theory is quoted shortly here. For details see [6]. Some basic steps which are necessary for understanding are outlined here.
Three different coordinate systems are used: an orthogonal Cartesian coordinate system (x,y,z) for the beam (fig. 5); the orthogonal coordinate system (n,s,x) for any plate segment (fig. 6); and a contour coordinate system s with s along the contour midplane line of the cross-section, starting from any selected origin (fig. 7) (note that the coordinate systems are different compared to [6]).

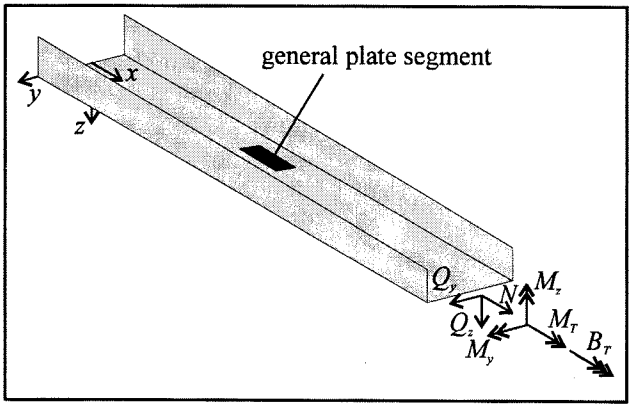

Fig. 5: Coordinate system of beam with generalized beam forces

The seven generalized beam forces are also shown in fig. 5. The torsional moment M_T consists of St.Venant Torsion T_S (warping unconstrained) and warping torsion T_ω (warping constrained) which is related to the warping bimoment B_T.

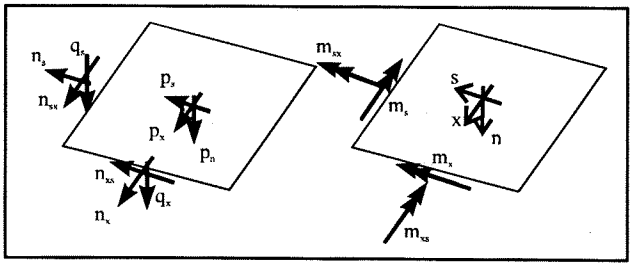

Fig. 6 Stress and moments resultants acting on any general plate segment and plate segment coordinate system

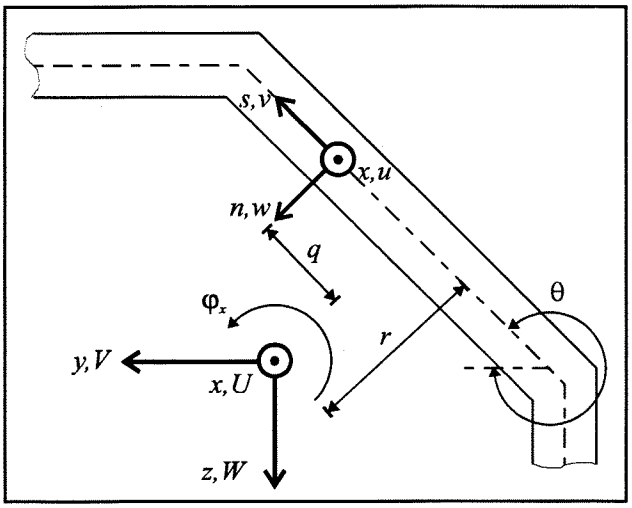

Fig. 7: Contour coordinate system and definitions of beam displacements and rotation

With kinematic correlation from geometric considerations in fig. 6 the plate displacements $v(x,s)$ and $w(x,s)$ will be related to the beam displacements V, W and φ_x. The axial displacement $u(x,s)$ is determined from the known shear strain-displacement relation. This results in the following equations:

$$\begin{aligned} u &= U + y\,\varphi_z + z\,\varphi_y + \omega\,\varphi_x' \\ v &= V\cos\theta + W\sin\theta + \varphi_x\, r \\ w &= -V\sin\theta + W\cos\theta + q\,\varphi_x \end{aligned} \qquad (9)$$

with

$$\omega = -\int_s r\,ds \quad ; \quad \varphi_y = \gamma_{xz} - W' \quad ; \quad \varphi_z = \gamma_{xy} - V'$$

Equations for the membrane strains ε_x and γ_{xs} and bending curvatures κ_x and κ_{xs} in the plate result:

$$\begin{aligned} \varepsilon_x &= U' + z\,\varphi_y' + y\,\varphi_z' + \omega\,\varphi_x'' \\ \gamma_{xs} &= \gamma_{xz}\sin\theta + \gamma_{xy}\cos\theta \\ \kappa_x &= \varphi_y'\cos\theta - \varphi_z'\sin\theta - q\,\varphi_x'' + \gamma_{xy}'\sin\theta - \gamma_{xz}'\cos\theta \\ \kappa_{xs} &= -2\,\varphi_x' \end{aligned} \qquad (10)$$

Note that the shear strain γ_{xs} will be taken into account.
The generalized beam forces and their equilibrium equations can be derived by applying the principle of virtual work similar to that used by Gjelsvik [10] but now including the transverse shear deformation of the beam. For this several energy distributions are developed:
a) The external work done by the shell and plate forces during a displacement of the cross-section:

$$W_e = \int_C \left(n_x u + n_{xs} v - m_x w' + q_x w - m_{xs}\varphi_x\right) ds + \sum_{\text{branches}} \left(m_{xs}^j w^j - m_{xs}^i w^i\right) \qquad (11)$$

or by substituting the kinematic relations of the displacements u, v and w from (9):

$$W_e = N\,U + Q_y V + Q_z W + M_T\varphi_x + B_T\varphi_x' + M_y\varphi_y + M_z\varphi_z + F_y\gamma_{xz} + F_z\gamma_{xy} \qquad (12)$$

with the generalized beam forces

$$
\begin{aligned}
N &= \int_s n_x\, ds \\
Q_y &= \int_s \left(n_{xs}\cos\theta - q_x \sin\theta\right) ds + \\
&\quad + \sum_{\text{branches}} \left(m_{xs}^{j}\sin\theta^{j} - m_{xs}^{i}\sin\theta^{i}\right) \\
Q_z &= \int_s \left(n_{xs}\sin\theta + q_x\cos\theta\right) ds - \\
&\quad - \sum_{\text{branches}} \left(m_{xs}^{j}\cos\theta^{j} - m_{xs}^{i}\cos\theta^{i}\right) \\
M_T &= \int_s \left(n_{xs} r - q_x q - m_{xs}\right) ds - \\
&\quad - \sum_{\text{branches}} \left(m_{xs}^{j} q^{j} + m_{xs}^{i} q^{i}\right) \\
B_T &= \int_s \left(n_x \omega - m_x q\right) ds \\
M_y &= \int_s \left(n_x z + m_x\cos\theta\right) ds \\
M_z &= \int_s \left(n_x y - m_x\sin\theta\right) ds \\
F_y &= -\int_s m_x\cos\theta\, ds \\
F_z &= \int_s m_x\sin\theta\, ds
\end{aligned}
\qquad (13)
$$

Important are the following known simplification [10]:

$$
Q_y = M_z' \;;\; Q_z = M_y' \;;\; M_T = T_S + T_\omega \;;\; T_\omega = -B_T'
$$

$$
T_S = -2\int_s m_{xs}\, ds \;;\; T_\omega = \int_s \left(n_{xs} r + \frac{\delta m_x}{\delta x} q\right) ds \qquad (14)
$$

b) the external virtual work done by the applied loadings on the plate:

$$
\begin{aligned}
w_e &= p\,U + q_y V + q_z W + m_T \varphi_x + b_T \varphi_x' + \\
&\quad + m_y \varphi_y + m_z \varphi_z + f_y \gamma_{xz} + f_z \gamma_{xy}
\end{aligned}
\qquad (15)
$$

p, q_y, q_z, m_T, b_T, m_y, m_z, f_y, and f_z are generalized load intensities on the beam, derived from loadings on the shell [10].

c) the strain energy using the relations between beam forces and shell forces:

$$
\begin{aligned}
\Pi &= \frac{1}{2}\left(N\,U' + T_S \varphi_x' + B_T \varphi_x'' + M_y \varphi_y + M_z \varphi_z + \right. \\
&\quad \left. + G_y \gamma_{xy} + G_z \gamma_{xz} + F_y \gamma_{xz}' + F_z \gamma_{xy}'\right)
\end{aligned}
\qquad (16)
$$

with

$$
G_y = \int_s n_{xs}\cos\theta\, ds \quad ; \quad G_z = \int_s n_{xs}\sin\theta\, ds \qquad (17)
$$

d) the internal virtual work which is obtained from strain energy can be simplified to:

$$
W_i = -T_S \varphi_x' - G_y \gamma_{xy} - G_z \gamma_{xz} \qquad (18)
$$

There are six equilibrium equations which are obtained between the acting generalized loads and the resulting beam forces by considering a beam element and equating the external work to internal work for any virtual displacement:

$$
\begin{aligned}
N' + p &= 0 \\
M_z'' + m_z' + q_y &= 0 \\
M_y'' + m_y' + q_z &= 0 \\
B_T'' + b_T' - T_S' - m_T &= 0 \\
F_z' + G_y &= 0 \\
F_y' + G_z &= 0
\end{aligned}
\qquad (19)
$$

The 9 generalized beam forces are related to the 6 generalized displacements. Using modified plate stress-strain relations (8) and plate strain-beam displacement relations (10) a system of differential equations can be derived:

$$
\begin{bmatrix} N \\ M_y \\ M_z \\ B_T \\ T_S \\ G_y \\ G_z \\ F_z \\ F_y \end{bmatrix} =
\begin{bmatrix}
K_{11}^* & K_{12}^* & K_{13}^* & K_{14}^* & K_{15}^* & K_{16}^* & K_{17}^* & K_{18}^* & K_{19}^* \\
 & K_{22}^* & K_{23}^* & K_{24}^* & K_{25}^* & K_{26}^* & K_{27}^* & K_{28}^* & K_{29}^* \\
 & & K_{33}^* & K_{34}^* & K_{35}^* & K_{36}^* & K_{37}^* & K_{38}^* & K_{39}^* \\
 & & & K_{44}^* & K_{45}^* & K_{46}^* & K_{47}^* & K_{48}^* & K_{49}^* \\
 & & & & K_{55}^* & K_{56}^* & K_{57}^* & K_{58}^* & K_{59}^* \\
 & & & & & K_{66}^* & K_{67}^* & K_{68}^* & K_{69}^* \\
 & & \text{symmetric} & & & & K_{77}^* & K_{78}^* & K_{79}^* \\
 & & & & & & & K_{88}^* & K_{89}^* \\
 & & & & & & & & K_{99}^*
\end{bmatrix}
\begin{bmatrix} U' \\ \varphi_y' \\ \varphi_z' \\ \varphi_x'' \\ \varphi_x' \\ \gamma_{xy} \\ \gamma_{xz} \\ \gamma_{xy}' \\ \gamma_{xz}' \end{bmatrix}
\qquad (20)
$$

The coefficients K_{ij}^* are given in the appendix.

For a beam made of general laminates having an unsymmetric cross-section the stiffness matrix [K^*] is completely populated. Some coefficients will be zero if any kind of symmetry is used relating to cross-section and stacking sequence of laminates and if the coordinate system is chosen judiciously.

C-beams under bending and torsional loads

Analytical solution

Three different composite GRP C-beams are chosen as specimens with identical geometry but different ply-stacking of the branches. Their geometric data are summed up in table 2, the cross-section is shown in fig. 8 with its point of reference laid at the intersection of cross-section contour-line with axis of symmetry.

Cases	Cross-section	Stacking
	flanges b = 30 mm	
C1	web h = 56 mm	$[+30/-30]_S$
C2	wall-thickness t =	$[+45/-45]_S$
C3	1.2 mm (4 layers)	$[+45]_4$

Load condition	Length l	Load
tip bending load	777 mm	Q = 19.8N
torsional load	800 mm	M_T =1.34Nm

Table 2: Geometric data of GRP-C-beams

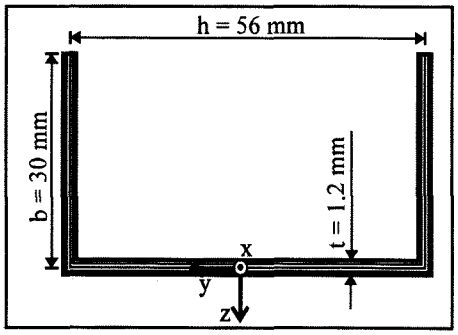

Fig. 8: Cross-section of C-beam with point of reference

There are two loading conditions considered (fig. 9). Tip bending load with free warping at the tip and a clamped end and torsional load at the middle section of the beam with fork bearings at both ends. The fork bearings take no forces in axial directions so warping is free. In the second case only half of the beam can be considered. Because of symmetry warping is constraint at the loaded middle section.

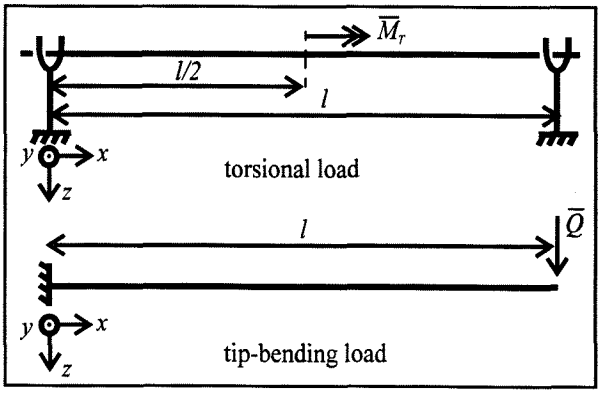

Fig. 9: Considered load conditions for GRP C-beams

Because of symmetric stacking sequences (all stiffness-coefficients B_{ij}^* are zero), the symmetric cross-section, and the chosen reference point the system of differential equations (20) reduces to:

$$\begin{bmatrix} N \\ M_y \\ M_z \\ B_T \\ T_S \\ G_y \\ G_z \\ F_z \\ F_y \end{bmatrix} = \begin{bmatrix} K_{11}^* & 0 & K_{13}^* & 0 & 0 & (K_{16}^*) & 0 & 0 & 0 \\ & K_{22}^* & 0 & K_{24}^* & 0 & 0 & (K_{27}^*) & K_{28}^* & 0 \\ & & K_{33}^* & 0 & K_{35}^* & 0 & 0 & 0 & K_{39}^* \\ & & & K_{44}^* & 0 & 0 & (K_{47}^*) & K_{48}^* & 0 \\ & & & & K_{55}^* & 0 & 0 & 0 & K_{59}^* \\ & & & & & K_{66}^* & 0 & 0 & 0 \\ & & \text{symmetric} & & & & K_{77}^* & 0 & 0 \\ & & & & & & & K_{88}^* & 0 \\ & & & & & & & & K_{99}^* \end{bmatrix} \begin{bmatrix} U' \\ \varphi_y' \\ \varphi_z' \\ \varphi_x'' \\ \varphi_x' \\ \gamma_{xy} \\ \gamma_{xz} \\ \gamma_{xy}' \\ \gamma_{xz}' \end{bmatrix} \quad (21)$$

The coefficients put in parenthesis are zero for C-beams C3. The remaining coefficients are given in the appendix.

Tip bending load. For the tip bending loaded C-beam the only acting load is:

$$q_z(l) = \bar{Q}_z$$

All other loads are zero.

For a beam subjected to tip bending or tip torsional load the variation of shear-strain is zero ($\gamma_{xy}' = \gamma_{xz}' = 0$). Comparing this with equilibrium equations (19) and the differential equation system of the C-beam (22) one can obtain:

$$\begin{aligned} N = 0 &\Rightarrow K_{11}^* U' + K_{13}^* \varphi_y' + K_{16}^* \gamma_{xy} = 0 \\ M_z = 0 &\Rightarrow K_{22}^* \varphi_z' + K_{24}^* \varphi_x'' + K_{27}^* \gamma_{xz} = 0 \\ M_y = \bar{Q}_z(x-l) &\Rightarrow K_{13}^* U' + K_{33}^* \varphi_y' + K_{35}^* \varphi_x' = \bar{Q}_z(x-l) \\ B_T' - T_S = 0 &\Rightarrow K_{24}^* \varphi_z'' + K_{44}^* \varphi_x''' - K_{35}^* \varphi_y' - K_{55}^* \varphi_x' = 0 \\ F_z' = G_y &\Rightarrow K_{28}^* \varphi_z'' + K_{48}^* \varphi_x''' = K_{16}^* U' + K_{66}^* \gamma_{xy} \\ F_y' = G_z &\Rightarrow K_{39}^* \varphi_y'' + K_{59}^* \varphi_x'' = K_{27}^* \varphi_z' + K_{47}^* \varphi_x'' + K_{77}^* \gamma_{xz} \end{aligned} \quad (22)$$

This system of six equations has to be solved with respect to a differential equation in φ_x and its derivatives by substitution. Because there are still seven unknown coefficients more equations are needed. One gets them by derivating N, M_y and M_z. Now there are three more equations and one more unknown coefficient U''':

$$\begin{aligned} N' = 0 &\Rightarrow K_{11}^* U'' + K_{13}^* \varphi_y' = 0 \\ M_z' = 0 &\Rightarrow K_{22}^* \varphi_z'' + K_{24}^* \varphi_x''' = 0 \\ M_y' = \bar{Q}_z &\Rightarrow K_{13}^* U'' + K_{33}^* \varphi_y'' + K_{35}^* \varphi_x'' = \bar{Q}_z \end{aligned} \quad (23)$$

The remaining differential equation of 3rd order is:

$$K_{A1} \varphi_x''' + K_{B1} \varphi_x'' + K_{C1} \varphi_x' + K_{D1} \bar{Q}_z(x-l) = 0 \quad (24)$$

The constants K_{ij} are functions of stiffness coefficients K_{ij}^*. With the help of the mathematical program MATHCAD 6.0 PLUS the differential equation has been solved by using the following boundary conditions:

Clamped end: $\varphi_x(x=0) = 0$

$\varphi_x'(x=0) = 0$ (warping constrained)

Loading end: $\varphi_x''(x=l) = 0$ (warping free)

Now the differential equations for other beam displacements can be achieved by substituting in (23). For φ_z' one can find in general form:

$$\varphi_y' = K_{A2} \varphi_x''' + K_{B2} \varphi_x'' + K_{C2} \varphi_x' + K_{D2} \bar{Q}_z(x-l) \quad (25)$$

Integrating (26) the bending slope φ_y can be determined. Remembering $W' = \gamma_{xz} - \varphi_y$ one can find the corresponding boundary conditions and the solution for the deflection W. For brevity the complete calculation is omitted here.

Torsion load. The acting torsion load at the middle section of the beam is:

$$m_T(l/2) = \bar{M}_T$$

With the same procedure described above for the bending load-case one gets a similar system of nine differential equations:

$$
\begin{aligned}
N = 0 &\Rightarrow K_{11}^{*} U' + K_{13}^{*} \varphi_y' + K_{16}^{*} \gamma_{xy} = 0 \\
M_z = 0 &\Rightarrow K_{22}^{*} \varphi_z' + K_{24}^{*} \varphi_x'' + K_{27}^{*} \gamma_{xz} = 0 \\
M_y = 0 &\Rightarrow K_{13}^{*} U' + K_{33}^{*} \varphi_y' + K_{35}^{*} \varphi_x' = 0 \\
B_T' - T_S = \bar{M}_T &\Rightarrow K_{24}^{*} \varphi_z'' + K_{44}^{*} \varphi_x''' - K_{35}^{*} \varphi_y' - K_{55}^{*} \varphi_x' = \bar{M}_T \\
F_z' = G_y &\Rightarrow K_{28}^{*} \varphi_z'' + K_{48}^{*} \varphi_x''' = K_{16}^{*} U' + K_{66}^{*} \gamma_{xy} \qquad (26) \\
F_y' = G_z &\Rightarrow K_{39}^{*} \varphi_y'' + K_{59}^{*} \varphi_x'' = K_{27}^{*} \varphi_z' + K_{47}^{*} \varphi_x'' + K_{77}^{*} \gamma_{xz} \\
N' = 0 &\Rightarrow K_{11}^{*} U'' + K_{13}^{*} \varphi_y' = 0 \\
M_z' = 0 &\Rightarrow K_{22}^{*} \varphi_z'' + K_{24}^{*} \varphi_x''' = 0 \\
M_y' = 0 &\Rightarrow K_{13}^{*} U'' + K_{33}^{*} \varphi_y'' + K_{35}^{*} \varphi_x'' = 0
\end{aligned}
$$

The remaining differential equation in φ_x is:

$$K_{A3} \varphi_x''' + K_{B3} \varphi_x'' + K_{C3} \varphi_x' + K_{D3} \bar{M}_T = 0 \qquad (27)$$

and the equation for deflection W is obtained in the same way as described above.

Finite-Element Analysis

To verify the analytical results a finite-element analysis was made using the program ANSYS. The C-beams were modelled with SHELL 91-elements, a layered 8 node shell-element. The flange width was divided into two elements, web height into three elements. For the bending load condition 294 elements were used (see fig. 10), for the torsion load condition 140 elements (only half of the beam is to be modelled).

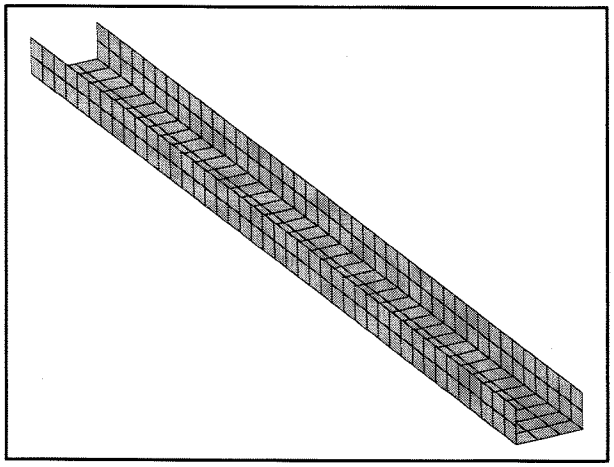

Fig. 10: Finite-element modell of composite C-beam

To take into account the restrictive assumption of rigid cross-section and neglecting stress and strain in contour-direction additional boundary conditions were used in the model. With a special command every cross-section of the C-beam spanned by nodes was defined as a rigid section. For free deformation of the beam, these conditions are not considered. Thus a comparsion of old and modified theory with finite-element analysis is possible.

Experimental Analysis

The analysed C-beams are made of the GRP material in table 1. The specimens were built by employing an auto-clave molding technique. Their laminated branches have identical stacking sequences. For that the fabrication of the specimen was simple by laying-up the glass-epoxy layers around a C-formed metal mold and compressing them by applying vacuum.

The three C-beams were tested separately for their structural response under tip bending load and torsional load at the middle section of the beam.

In fig. 11 the set-up for bending test is shown. For secure clamping at one end a special device was built. At the tip the web was reinforced with a small stiff plate for spreading the load. The load is obtained by using weights. In order to avoid buckling in the flanges the bending load was applied in the positive z-direction. The structural response was measured in terms of bending and induced twist at the tip. These were determined by measuring the displacements of the cross-section by means of two electronic detectors positioned in contact with one point of the contour line via a support plate.

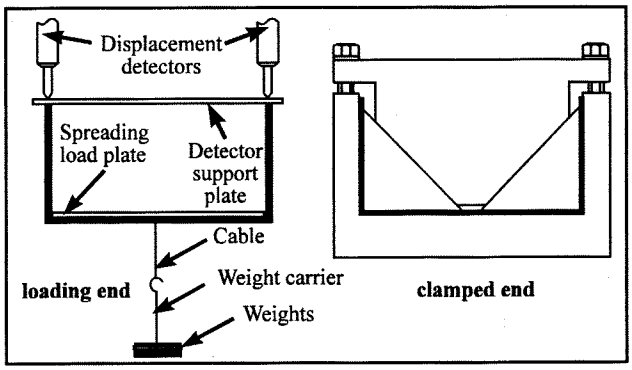

Fig. 11: Bending test set-up

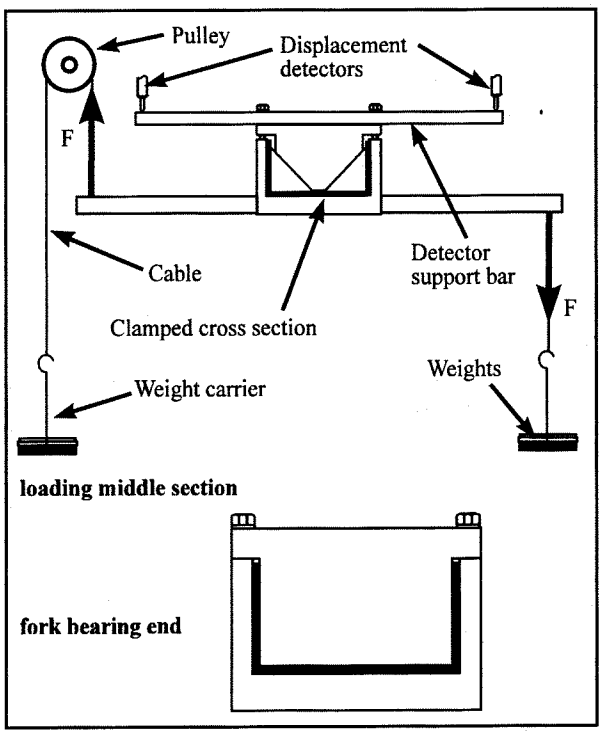

Fig. 12: Torsion test set-up

Fig. 12 shows the set-up for torsion test. At both ends fork bearings are used which allow warping. The torsion load was obtained by two weights, one via a pulley. For measuring displacements the same set-up was used like as with the bending test.

Results and Discussion

In the following six figures the results for the three different GRP C-beams and the two load conditions are given. The spanwise plots of both analytical solutions (theory of Chandra and Chopra[6] typed as theory a, modified theory as theory b), the solutions of finite-element analysis (with boundary condition rigid cross-sections typed as FE a, free deformation of cross-sections as FE b) and the experimental result at the loading points are shown.

First of all it is to be noted that there is a clear difference between both theories. The theory by Chandra and Chopra[6] implies a too high a stiffness. The results of the finite-element-analysis correspond very well with the respective theory for the C-beams with the stackings $[+30/-30]_S$ and $[+45/-45]_S$, and well with the stacking $[+45]_4$ at least with the modified theory. By choosing the correct boundary conditions the finite-element-method allows a good simulation of such restrictive theories.

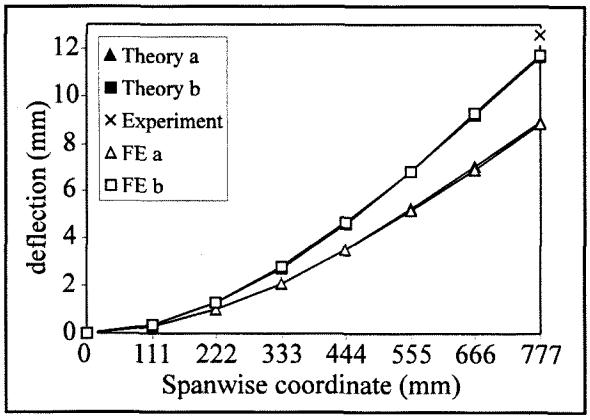

Fig. 13: Deflection of tip bending loaded GRP C-beam C1 with stacking $[+30/-30]_S$

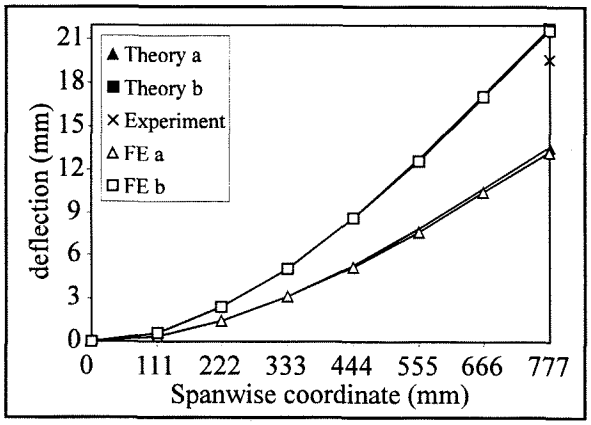

Fig. 14: Deflection of tip bending loaded GRP C-beam C2 with stacking $[+45/-45]_S$

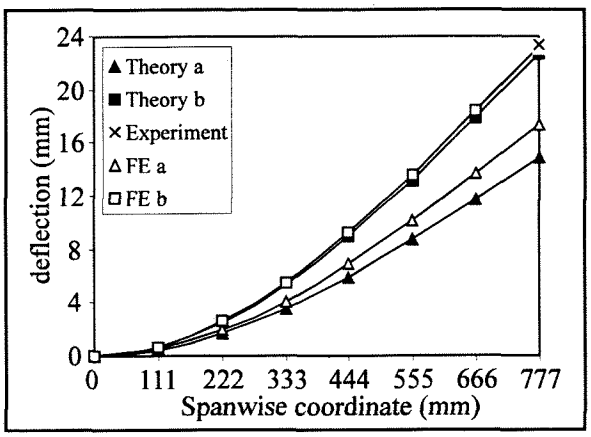

Fig. 15: Deflection of tip bending loaded GRP C-beam C3 with stacking $[+45]_4$

The experimental results correspond with the modified theory in spite of small differences. The bending and torsional stiffness decreases from stacking $[+30/-30]_S$ via $[+45/-45]_S$ to $[+45]_4$ as expected.

In spite of branches containing elastic couplings because of their laminate stacking, no significant coupled deformation (twist at bending load or deflection at torsion load) could be noticed. The reason for this is the special geometry of the C-beam that allows no geometric coupling. The CRP I-beam analysed in [6] has a clear bending-torsion coupling because of the distance between the anisotropic flanges. They lay perpendicular to the load direction and thus cause the bending torsion coupling. In case of C-beam only the web lays perpendicular to the load direction. Both flanges are too stiff and constrain the coupling of the web.

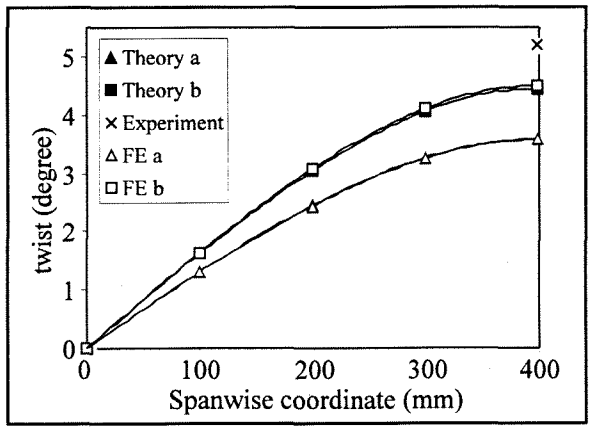

Fig. 16: Twist of warping torque loaded GRP-C-beam C1 with stacking $[+30/-30]_S$

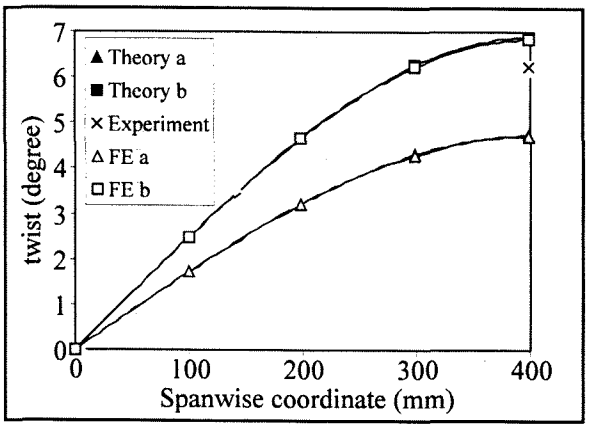

Fig. 17: Twist of warping torque loaded GRP C-beam C2 with stacking $[+45/-45]_S$

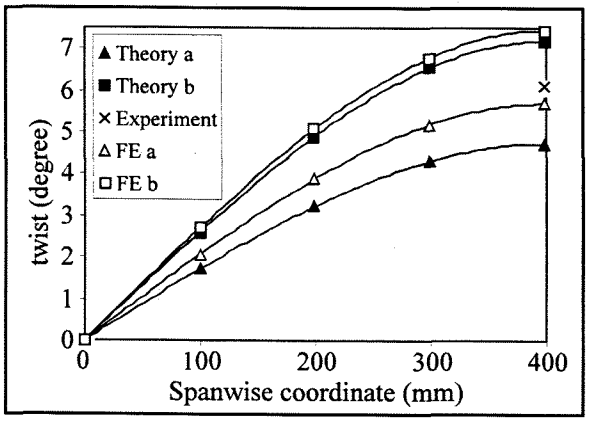

Fig. 18: Twist of warping torque loaded GRP C-beam C3 with stacking $[+45]_4$

The almost exact confirmation of the modified theory by the finite-element analysis with C-beams that have stackings of $[+30/-30]_S$ and $[+45/-45]_S$ is an indication for the importance of the inplane deformation behaviour of thin-walled beams. With the modified plate stress field (8) it is possible to take into account these inplane-warping effects. The limitations of the modified theory can be seen in fig. 15 and 18 showing the results for the C-beam with stacking of $[+45]_4$. The deviation between analytical and finite-element results is caused by high tension-shear coupling of the single branches. Because of this the low inplane stiffness perpendicular to the fibre orientation can not be taken into account, even with the modified theory. Here a nonlinear procedure is necessary.

Conclusion

The theory by Chandra and Chopra[6] for linear analysis of thin-walled beams with open cross-section made of general composite laminates (thus containing elastic couplings) is modified to take into account the inplane-deformation of cross-section. The effects of elastic coupling range from inplane couplings of laminates to couplings of beam displacements because of beam geometry and have a significant influence on the inplane-deformation. Finite-element-analysis as well as experimental results confirm the modified theory and at the same time show its limitations. Especially laminated beams with no or low proportion of fibres in axial direction can be exactly calculated with the modified theory. Beams containing segments of laminates with a high inplane coupling can not be exactly calculated, even with the modified theory.

References

(1) Bank, L. C. and Kao, C. H.
"The Influence of Geometric and Material Design Variables on the Free Vibration of Thin-Walled Composite Material Beams"
Journal of Vibration, Acoustics, Stress, and Reliability in Design, Vol. 111, July 1989

(2) Librescu, L., Meirovitch, L. and Song, O.
"A Refined Structural Model of Composite Aircraft Wings for the Enhancement of Vibrational and Aeroelastic Response Characteristics"
AIAA-93-1536-CP

(3) Bothwell, Ch. M., Chandra, R., Chopra, I.
"Torsional Actuation with Extension-Torsion Composite Coupling and a Magnetostrictive Actuator"
AIAA Journal, Vol. 33, No. 4, April 1995

(4) Bauld jr., N. R. and Lih-Shyng T.
"A Vlasov Theory for Fiber-Reinforced Beams with Thin-Walled open Cross Sections"
Int. J. Solids Structures, Vol. 20, No. 3, 1984

(5) Vlasov, V. Z.
"Thin-Walled Elastic Beams"
National Science Foundation and Department of Commerce, USA

(6) Chandra, R. and Chopra I.
"Experimental and Theoretical Analysis of Composite I-Beams with Elastic Couplings"
AIAA Journal, Vol. 29, No. 12, December 1991

(7) Chandra, R. and Chopra, I.
"Structural Modeling of Composite Beams with Induced-Strain Actuators"
AIAA Journal, Vol. 31, No. 9, September 1993

(8) Wu, X. and Sun C. T.
"Simplified Theory for Composite Thin-Walled Beams"
AIAA Journal, Vol. 30, No. 12, December 1992

(9) Kaiser, C. and Francescatti, D.
"Some basic reflections on elastic couplings of composite beams"
Proc. of the Symposium *Calculation of Composite Structures using Numerical Methods*, Technical University Munich, Chair for Lightweight Structures, March 1996 (in German)

(10) Gjelsvik, A.
"The Theory of Thin-Walled Bars"
John Wiley & Sons, New York, 1981

(11) Laulusa, A., Bachau, O. A. and Theron, N. J.
"Theoretical and Experimental Investigation of the Nonlinear Behavior of Composite Beams"
La Recherche Aérospatiale, No. 4, 1995

Appendix

The elements of the stiffness matrix [*ABD*] of general plate stress field are calculated with classical laminate theory as follows:

$$A_{ij} = \sum_{k=1}^{m} C_{ij}^{k} \left(h_{k+1} - h_k \right)$$

$$B_{ij} = \frac{1}{2} \sum_{k=1}^{m} C_{ij}^{k} \left(h_{k+1}^2 - h_k^2 \right)$$

$$D_{ij} = \frac{1}{3} \sum_{k=1}^{m} C_{ij}^{k} \left(h_{k+1}^3 - h_k^3 \right)$$

C_{ij}^{k} refers to stiffness matrix of k^{th} layer of any laminated plate segment containing m layers with h_{k+1} and h_k as its coordinates in n-direction from midplane of laminate.

The coefficients of symmetric stiffness matrix [K^*] ($K_{ij}^{*} = K_{ji}^{*}$) will be calculated with stiffnesses A_{ij}^{*}, B_{ij}^{*} and D_{ij}^{*} from (9):

$K_{11}^{*} = \int_s A_{11}^{*}\, ds$; $K_{12}^{*} = \int_s (y A_{11}^{*} - B_{11}^{*} \sin\theta)\, ds$

$K_{13}^{*} = \int_s (z A_{11}^{*} + B_{11}^{*} \cos\theta)\, ds$; $K_{14}^{*} = \int_s (\omega A_{11}^{*} - B_{11}^{*} q)\, ds$;

$K_{15}^{*} = -2 \int_s B_{13}^{*}\, ds$; $K_{16}^{*} = \int_s A_{13}^{*} \cos\theta\, ds$;

$K_{17}^{*} = \int_s A_{13}^{*} \sin\theta\, ds$; $K_{18}^{*} = \int_s B_{11}^{*} \sin\theta\, ds$;

$K_{19}^{*} = -\int_s B_{11}^{*} \cos\theta\, ds$;

$K_{22}^{*} = \int_s \left[y (y A_{11}^{*} - B_{11}^{*} \sin\theta) - \sin\theta (y B_{11}^{*} - D_{11}^{*} \sin\theta) \right] ds$;

$K_{23}^{*} = \int_s \left[y (z A_{11}^{*} + B_{11}^{*} \cos\theta) - \sin\theta (z B_{11}^{*} + D_{11}^{*} \cos\theta) \right] ds$;

$K_{24}^{*} = \int_s \left[y (\omega A_{11}^{*} - B_{11}^{*} q) - \sin\theta (\omega B_{11}^{*} - D_{11}^{*} q) \right] ds$;

$K_{25}^{*} = -2 \int_s (y B_{13}^{*} - D_{13}^{*} \sin\theta)\, ds$;

$K_{26}^{*} = \int_s (y A_{13}^{*} \cos\theta - B_{31}^{*} \sin\theta \cos\theta)\, ds$;

$K_{27}^{*} = \int_s (y A_{13}^{*} \sin\theta - B_{31}^{*} \sin^2\theta)\, ds$;

$K_{28}^{*} = \int_s (y B_{11}^{*} \sin\theta - D_{11}^{*} \sin^2\theta)\, ds$;

$K_{29}^{*} = -\int_s (y B_{11}^{*} \cos\theta - D_{11}^{*} \sin\theta \cos\theta)\, ds$;

$K_{33}^{*} = \int_s \left[z (z A_{11}^{*} + B_{11}^{*} \cos\theta) + \cos\theta (z B_{11}^{*} + D_{11}^{*} \cos\theta) \right] ds$;

$K_{34}^{*} = \int_s \left[z (\omega A_{11}^{*} - B_{11}^{*} q) + \cos\theta (\omega B_{11}^{*} - D_{11}^{*} q) \right] ds$;

$K_{35}^{*} = -2 \int_s (z B_{13}^{*} + D_{13}^{*} \cos\theta)\, ds$;

$K_{36}^{*} = \int_s (z A_{13}^{*} \cos\theta + B_{31}^{*} \cos^2\theta)\, ds$;

$K_{37}^{*} = \int_s (z A_{13}^{*} \sin\theta + B_{31}^{*} \sin\theta \cos\theta)\, ds$;

$K_{38}^{*} = \int_s (z B_{11}^{*} \sin\theta + D_{11}^{*} \sin\theta \cos\theta)\, ds$;

$K_{39}^{*} = -\int_s (z B_{11}^{*} \cos\theta + D_{11}^{*} \cos^2\theta)\, ds$;

$K_{44} = \int_s \left[\omega (\omega A_{11}^{*} - B_{11}^{*} q) - q (\omega B_{11}^{*} - D_{11}^{*} q) \right] ds$;

$K_{45}^{*} = -2 \int_s (\omega B_{13}^{*} - D_{13}^{*} q)\, ds$;

$K_{46}^{*} = \int_s \cos\theta (\omega A_{13}^{*} - B_{31}^{*} q)\, ds$;

$K_{47}^{*} = \int_s \sin\theta (\omega A_{13}^{*} - B_{31}^{*} q)\, ds$;

$K_{48}^{*} = \int_s (\omega B_{11}^{*} \sin\theta - D_{11}^{*} q \sin\theta)\, ds$;

$K_{49}^{*} = -\int_s (\omega B_{11}^{*} \cos\theta - D_{11}^{*} q \cos\theta)\, ds$;

$K_{55}^{*} = 4 \int_s D_{33}^{*}\, ds$; $K_{56}^{*} = -2 \int_s B_{33}^{*} \cos\theta\, ds$;

$K_{57}^{*} = -2 \int_s B_{33}^{*} \sin\theta\, ds$; $K_{58}^{*} = -2 \int_s D_{13}^{*} \sin\theta\, ds$;

$K_{59}^{*} = 2 \int_s D_{13}^{*} \cos\theta\, ds$;

$K_{66}^{*} = \int_s A_{33}^{*} \cos^2\theta\, ds$; $K_{67}^{*} = \int_s A_{33}^{*} \sin\theta \cos\theta\, ds$;

$K_{68}^{*} = \int_s B_{31}^{*} \sin\theta \cos\theta\, ds$; $K_{69}^{*} = -\int_s B_{31}^{*} \cos^2\theta\, ds$;

$K_{77}^{*} = \int_s A_{33}^{*} \sin^2\theta\, ds$; $K_{78}^{*} = \int_s B_{31}^{*} \sin^2\theta\, ds$;

$K_{79}^{*} = -\int_s B_{31}^{*} \sin\theta \cos\theta\, ds$;

$K_{88}^{*} = \int_s D_{11}^{*} \sin^2\theta\, ds$; $K_{89}^{*} = -\int_s D_{11}^{*} \sin\theta \cos\theta\, ds$;

$K_{99}^{*} = \int_s D_{11}^{*} \cos^2\theta\, ds$.

For the analysed C-beams the stiffness coefficients K_{ij}^{*} can be calculated to:

$K_{11}^{*} = (2b + h) A_{11}^{*}$; $K_{13}^{*} = b^2 A_{11}^{*}$; $K_{16}^{*} = h A_{13}^{*}$

$K_{22}^{*} = \frac{h^2}{2} \left(b + \frac{h}{6} \right) A_{11}^{*}$; $K_{24}^{*} = -\frac{h^2 b^2}{4} A_{11}^{*} - b^2 D_{11}^{*}$

$K_{27}^{*} = b h A_{13}^{*}$; $K_{28}^{*} = -2 b D_{11}^{*}$

$K_{33}^{*} = \frac{2}{3} b^3 A_{11}^{*} + h D_{11}^{*}$

$K_{35}^{*} = -2 h D_{13}^{*}$; $K_{39}^{*} = -h D_{11}^{*}$

$K_{44}^{*} = \frac{h^2 b^3}{6} A_{11}^{*} + \left(\frac{h^3}{12} + \frac{2}{3} b^2 \right) D_{11}^{*}$

$K_{47}^{*} = -\frac{h b^2}{2} A_{13}^{*}$; $K_{48}^{*} = b^2 D_{11}^{*}$

$K_{55}^{*} = 4 (2b + h) D_{33}^{*}$; $K_{59}^{*} = h D_{13}^{*}$; $K_{66}^{*} = h A_{33}^{*}$

$K_{77}^{*} = 2 b A_{33}^{*}$; $K_{88}^{*} = 2 b D_{11}^{*}$; $K_{99}^{*} = h D_{11}^{*}$